Full Text View

Volume 32, Issue 12 (December 2002)

Journal of Physical Oceanography
Article: pp. 3474–3489 | Abstract | PDF (2.48M)

Seasonal Heat Budgets of the North Pacific and North Atlantic Oceans

Jiande Wang* **and James A. Carton**

Department of Meteorology, University of Maryland at College Park, College Park, Maryland

(Manuscript received February 21, 2001, in final form May 31, 2002)

DOI: 10.1175/1520-0485(2002)032<3474:SHBOTN>2.0.CO;2

ABSTRACT

Here, seasonal heat transport in the North Pacific and North Atlantic Oceans is compared using a 49-year-long analysis based on data assimilation. In midlatitudes surface heat flux is largely balanced by seasonal storage, while equatorward of 15°N, divergence of heat transport balances seasonal storage. The seasonal cycle of heat transport in the Pacific is in phase with the annual migration of solar radiation, transporting heat from the warm hemisphere to the cool hemisphere. Analysis shows that the cycle is large with peak-to-peak shifts of 5 PW. To examine the cause of these large shifts, a vertical and zonal decomposition of the heat budget is carried out. Important contributions are found from the annual cycle of wind drift in the mixed layer and adiabatically compensating return flow, part of the vigorous shallow tropical overturning cell. The annual cycle of heat transport in the North Atlantic is also large. Here too, wind-driven transports play a role, although not as strongly as in the Pacific, and this is an important reason for the differences in heat transport between the basins. Analysis shows the extent to which seasonally varying geostrophic currents and seasonal diabatic effects are relatively more important in the Atlantic. Thus, although the annual cycle of zonally integrated mass transport in the mixed layer is only 1/5 as large, the time-averaged heat transport is nearly as large as in the Pacific. This difference in transport mechanics gives rise to changes in the phase of seasonal heat transport with latitude in the Atlantic.

1. Introduction

The seasonal variations of temperature and velocity in the North Pacific and Atlantic share many features in common. Both have prominent seasonally varying North Equatorial Countercurrents. Both are subject to westerly winds in midlatitudes whose intensity increases significantly in winter, with corresponding increases in Ekman transport and seasonally varying western boundary currents. And in both oceans the mixed layers undergo pronounced seasonal variations in response to changes in winds and heating. Yet, the time-averaged heat and mass transport are fundamentally different in the two basins

since the North Atlantic has a much more vigorous deep thermohaline circulation (Hall and Bryden 1982; Molinari et al. 1990) while the Pacific has a stronger shallow tropical overturning cell (Johnson and McPhaden 1999; Johnson 2001). In this shallow cell water transported poleward in the mixed layer is replaced by water subducting in the interior subtropics, which then travels equatorward by western boundary and interior pathways. In this study we examine the seasonal cycles of the heat budget in the two oceans for differences due to differences in the circulation.

One important term in the heat budget of the oceans is the seasonally varying meridional heat transport ($C_p\rho \int\int vT\, dx\, dz$). Heat transport is accomplished by compensating volume transports of warm and cool water that can be carried out in various ways. Kraus and Levitus (1986), for example, examine seasonal wind-driven Ekman transport assuming this warm surface flow is compensated for by a uniform cool return flow at depth. Since the difference in temperature between the surface and deep flows is large, this assumption leads to estimates of the compensated Ekman contribution that account for 50% or more of the total seasonal meridional heat transport in the Tropics. The Kraus and Levitus assumption is supported by model-based estimates of Böning and Hermann (1994) and Jayne and Marotzke (2001). Indeed, in a comprehensive study of a high-resolution model Jayne and Marotzke (2001) note that the seasonal cycle projects more effectively on the barotropic mode than the baroclinic mode outside of the Tropics, and thus one might anticipate that at seasonal periods Ekman transport would be compensated for by weak depth-averaged flow.

However, Bryden et al. (1991) and Wijffels et al. (1996) point to the absence of an observed seasonal cycle in deep Pacific transport expected if compensation were occurring at those levels. Bryden and Hall (1980) suggest that compensating flows occur within the thermocline gyre itself along 25°N (at least for the time-mean case). Alternatively, Philander and Pacanowski (1986) argue that the dominant seasonal balance in the heat budget is between horizontal advection by geostrophic currents and storage in the ridge–trough system of the equatorial thermocline with little compensating deep flow. Thus, in addition to the time-average heat transport we are interested in examining the relative importance of advection, local storage, surface fluxes, and wind-driven transport in contributing to seasonal heat transport.

This study has been made possible by the availability of a global reanalysis of temperature, salinity, and currents covering the period 1950–98 (Carton et al. 2000a,b). The reanalysis uses all available temperature and salinity observations from the World Database 1994 (WDB-94: Levitus and Antonov 1997), satellite altimetry, and sea surface temperature observations to constrain a numerical model of the primitive equations of motion. Because this analysis consists of uniformly gridded fields that span the global oceans in a way that is consistent with available information, we are able to examine the full heat balance in comparison with the ocean's mass balance.

Use of this analysis has several advantages over alternative direct and indirect approaches. In the direct method of computing meridional heat transport, pioneered by Jung (1952) and exploited by Hall and Bryden (1982), Fillenbaum and Lee (1997), Roemmich et al. (2001), and others, heat transport is estimated directly from observations of temperature and geostrophic plus Ekman current. Unfortunately, limits on data coverage restrict the geographic lines and seasons where direct estimates of heat transport can be made. Numerical model simulations have also been used to calculate meridional heat transport, which have full basin coverage, but are subject to large, poorly understood errors (Bryan 1962; Böning and Herrmann 1994).

In the indirect method, introduced in a groundbreaking study by Oort and Vonder Haar (1976), oceanic heat transport is estimated as the residual needed to close the global energy balance based on atmospheric or surface flux measurements. Applying this approach to the calculation of meridional heat transport requires integrating the difference between the net surface heat flux and the local rate of heat storage meridionally between latitudinal circles. This integral is generally begun at a polar latitude where the transport is assumed small. Errors introduced by the differencing and integration steps likely explain the large discrepancies between direct and indirect seasonal heat transport estimates in the Atlantic (evident in comparing the results of Lamb and Bunker 1982; Philander and Pacanowski 1986; Hsiung et al. 1989; Molinari et al. 1990). Although recent studies such as Trenberth and Caron (2001) have reduced the problem, inconsistencies persistent in attempts to calculate seasonal heat transport in the Atlantic using the indirect approach are additional motivations for the current study.

2. Data

The monthly Simple Ocean Data Assimilation (SODA) analysis of Carton et al. (2000a,b) spans the full period 1950–98. The analysis software uses a multivariate version of optimal interpolation in which the temperature and salinity fields are analyzed using a multivariate form of statistical objective analysis. The temperature and salinity database include data from WDB-94, XBT data from the National Oceanographic Data Center archive, the National Center Environmental Prediction analysis database, the Tropical Atmosphere–Ocean array, and the SST data of Reynolds and Smith (1994). Satellite altimeter sea level from Geosat, *ERS-1*, and TOPEX/Poseidon is used in the decades of the 1980s and 1990s. Data checking for this analysis includes checks for duplicate reports and errors in the recorded position and time of observations, static stability, deviation from climatology, and checks on the relationship between temperature and salinity by comparison with historical temperature/salinity relationships.

The forecast model uses the Geophysical Fluid Dynamics Laboratory Modular Ocean Model 2.b numerics driven by Combined Ocean–Atmosphere Data Set (COADS) winds (da Silva and Levitus 1994), with conventional choices for mixing, and so on. Climatological surface heat flux is specified as well since the surface flux is not well determined [Gleckler and Weare (1997) and Trenberth and Caron (2001) cite errors of 25–30 W m^{-2}]. The updating procedure will modify the temperature field, thus introducing an additional source term into the temperature equation reflecting the difference between column integrated heat transport divergence and local storage. Vertically integrated, this source term is often larger than the specified surface flux. Thus, we will interpret the source term throughout this study as a correction to surface heat flux.

The domain of this analysis is global (62°N–70°S) with 2.5° × 2.0° resolution in midlatitudes reducing to 2.5° × 0.5° in the Tropics (in the band of latitudes between 7° and 13°N/S the average meridional resolution is 0.8°). A sponge layer in the Arctic relaxes temperature and salinity to their climatological seasonal values, thus ensuring a reasonable rate, approximately 20 Sv (Sv $\equiv 10^6$ m^3 s^{-1}), of deep-water formation. Temperature, salinity, and sea level error covariances are basin-, depth- and latitude-dependent based on statistical studies of forecast errors. The zonal and meridional correlation scales are derived from an analysis of temperature observation minus forecast differences (see Carton et al. 2000a,b for a discussion of these). Near the surface in the Tropics the correlation scales are 450 and 250 km, smoothly approaching a uniform 375 km in midlatitudes, and decreasing somewhat with depth. The coarse resolution of this analysis means that mesoscale (and smaller) processes are unresolved. The analysis update cycle is 10 days, but uses a continuous updating algorithm to reduce the introduction of spurious variability. The results shown here are based on monthly averages of the 10-day spaced analyses. Comparisons to independent observations and to other ocean analyses are presented in Chepurin and Carton (1999) and Carton et al. (2000a,b).

The climatological monthly cycle of each term has been computed by averaging over 49 Januarys, Februarys, etc. No attempt has been made to remove the effects of interannual variability such as ENSO on the seasonal cycle. The instrument types and distributions have changed during the 49-yr period. To investigate the stability of the results, as well as the possibility of significant changes in the seasonal cycle over time, we have repeated some of our calculations independently for the first and second halves of the time period (discussed later). The differences are ~ 10%.

The heat budget, really an equation for conservation of potential temperature, includes local storage ($\partial\theta/\partial t$), divergence of horizontal transport [$\nabla_h \cdot (\mathbf{V}\theta)$], processes involved in the vertical redistribution of heat

$$\left[\frac{\partial(w\theta)}{\partial z} - A_v(z)\frac{\partial^2\theta}{\partial z^2}\right],$$

surface flux (Q), and horizontal eddy diffusion ($K_h\nabla^2{}_h\theta$)

$$\frac{\partial\theta}{\partial t} + \nabla_h\cdot(\mathbf{V}\theta) + \left[\frac{\partial(w\theta)}{\partial z} - A_v(z)\frac{\partial^2\theta}{\partial z^2}\right] = \frac{Q\delta(z)}{\rho_o C_p} + K_h\nabla_h^2\theta, \qquad (1)$$

where θ is the potential temperature, and $\mathbf{V}$ and w are horizontal and vertical currents, respectively. For these calculations ρ_o and C_p have been assumed to be constants with values of 1023 kg m^{-3} and 4186 J kg^{-1} K^{-1}, respectively. When this equation is averaged zonally from coast to coast, vertically from the bottom to the surface, and in time over multiple decades all terms drop out except the divergence of meridional transport, $\partial(v\theta)/\partial y$, on the left and

$$\frac{Q\delta(z)}{\rho_o C_p} + k_h\nabla_h^2\theta$$

on the right.

Mean meridional heat transports for the two ocean basins are presented in Figs. 1a and 1b. In the Atlantic our estimate of mean meridional heat transport is a bit lower than previous estimates south of 30°N. From the seasonal mean mass transport in the Atlantic (Fig. 2 left panel) we note that although the reanalysis has a vigorous overturning cell that

exceeds 21 Sv, consistent with the modeling studies of Böning and Herrmann 1994 and Yu and Malanotte-Rizzoli (1998), much of this water upwells within the North Atlantic and less than 6 Sv crosses the equator into the Southern Hemisphere (much less than the 13–14 Sv estimated by Schmitz and Richardson 1991). Böning et al. (1996) point out that a 2 Sv increase in the overturning strength corresponds to a 0.1 PW increase in heat transport.

The cause of this problem in our analysis is related to coarse vertical resolution in the deep ocean and insufficient production of Mediterranean Water that allows North Atlantic Deep Water to rise to unrealistically shallow levels and to mix. A similar problem was detected in other ocean GCM simulations (Böning et al. 1995). This problem is less serious in the Pacific, which has no significant deep-water production (although there is some northward deep flow, Fig. 3). The drop in northward heat flux in the Pacific between 25° and 30°N (Fig. 1b) results from a strong surface flux of heat out of the ocean in the west, which may well be a result of our coarse numerical resolution.

The mean circulations in both basins are dominated by anticyclonic subtropical gyres and cyclonic subarctic gyres. Between the coast of the United States and Bermuda (32°N, 64°W) our analysis shows a barotropic transport of 24 Sv, with a seasonal variation of 6 Sv. The mean estimates may be 10%–20% lower than some previous estimates (Holland and Bryan 1994; Yu and Malanotte-Rizzoli 1998; Baringer and Larsen 2001). The North Pacific is characterized by a stronger subtropical gyre circulation (36 Sv between Japan and 160°E along the 30°N latitude circle). The results of Kamenkovich et al. (2000) suggest that increasing horizontal resolution will accelerate the horizontal gyre and thus increase heat transport associated with gyre circulation (see Fig. 1b).

The annual cycle of barotropic volume transport is shown in Fig. 4 as the winter minus summer difference. In the tropical Atlantic there is a strong 12 Sv annual cycle in zonal transport associated with the boreal summer intensification of the North Equatorial Countercurrent. Transport in the North Equatorial Countercurrent of the eastern tropical Pacific is similar in magnitude to the Atlantic (approximately 12 Sv), but stronger in the west. The annual cycle of the subtropical gyre in the Atlantic, in contrast, is only 1/3 to 1/4 of the corresponding gyre in the Pacific.

The seasonal heat budget estimates are subject to a variety of errors including analysis errors due to model deficiencies (including errors in surface fluxes), measurement errors, and the inability of the observation suite to represent the key spatial and temporal scales of motion. The representativeness error has been raised in a few recent studies. Bryden et al. (1991) identify unresolved eddy fluxes as a major source and suggest an eddy heat flux component error on the order of 0.1 PW in the middle of the North Pacific subtropical gyre (~ 14% of the total). In an examination of heat transport using repeat zonal hydrographic sections with corresponding winds and SST Roemmich et al. (2001) point out the difficulty in getting a stable estimate of heat transport using one-time transects. Indeed, they find fluctuations of 50% in the subtropical Pacific during the 6-yr period 1993–99.

The large 0.76 PW estimate of northward heat transport by Bryden et al. (1991) at 24°N in the North Pacific, based on data from a single cruise, may illustrate the latter problem. Although our time mean estimate at this latitude is much lower (0.28 PW), we obtain a more similar 0.61 PW for the particular months, April–May 1985, for which his temperature data is available and a stronger gyre transport than usual (although as a reviewer points out, Bryden relied on climatological seasonal winds in this estimate, so the improved agreement using the actual monthly data may be fortuitous). Interestingly, the estimate based on a numerical simulation by Wilkin et al. (1995) is only one-half of the Bryden et al. (1991) estimate.

Among model errors, a key source will turn out to be wind stress. This error, in turn is a complex function of the surface meteorological observation distribution (most shipboard observations are confined to shipping lanes), their accuracies, and the accuracy of the bulk formula used to compute wind stress. An examination by Blanc (1985) suggests that errors in the bulk formula alone may lead to discrepancies that are as much as 45% of the average stress estimates in the North Atlantic. Other studies, for example, Roemmich et al. (2001), show much lower error estimates where direct measurements are available. Examination of the dependence of seasonal heat transport estimates on the choice of wind products by Jayne and Marotzke (2001) suggests errors of 0.5 PW in the subtropics of each basin increasing to 1 PW or more close to the equator (with the increase due to the increasing magnitude of Ekman transports at low latitudes).

In this study we assume that the representativeness error, along with the random component of the model and measurement errors, can be roughly estimated by the standard error of the monthly estimates about the climatological seasonal cycle (indicated by shading in Fig. 1) based on the assumption that each year's estimate is independent. This approach does not include error due to bias, something that is difficult to quantify (except through comparison with independent estimates).

3. Results

The seasonal heat budget is presented in Fig. 5. The lower panels present heat storage (time rate of change of heat content) and divergence of heat transport as a function of latitude and month. The sum of these terms gives our estimate of surface heat flux (positive values indicate a flux into the ocean). This sum is the zonally and vertically integrated model/data

temperature misfit plus climatological mean heat flux. Thus it is the amount of heat that the assimilation requires to be added to or subtracted from the ocean to be reasonably consistent with the equations of motion and the observations (i.e., the surface heat flux). The top panel shows an estimate of surface heat flux based on SST and a suite of meteorological observations based on the COADS analysis of da Silva and Levitus (1994) and is thus largely independent of our heat flux estimate (except for the use of SST. See also Hsiung et al. 1989 for an alternative surface heat flux analysis).[1] The corresponding standard error estimates are shown in Fig. 6. The results show a standard error of divergence of heat transport of approximately 10% of the seasonal cycle in the Tropics, increasing to 20% in midlatitudes. The uncertainty in heat storage is 20% in the Tropics, decreasing to low values in midlatitudes, where the hemispheric-scale effects of seasonal heating dominate. Still, despite the uncertainties, we proceed to address the causes of these balances, as they appear in this analysis.

Throughout the midlatitudes our reanalysis surface heat flux is into the ocean from April to September, and out of the ocean for the remainder of the year. However, in the Tropics the behavior of surface heat flux changes. In the Pacific close to, and just south of, the equator the analysis heat flux as well as the COADS heat flux is into the ocean throughout the year. The reanalysis and COADS surface heat fluxes differ in a narrow band of latitudes between 5°–10°N where COADS indicates a net flux of heat into the ocean throughout the year while the reanalysis indicates a narrow 5° band of latitude in which heat is being pumped out of the ocean (Fig. 5b). The longitudinal extend of this band spans the range 140°E–120° W. This narrow band shifts northward in summer following the northward shift of the intertropical convergence zone (ITCZ). Possible explanations for the existence of this band include cloud-induced solar shading within the ITCZ and enhanced latent heat loss on its northern edge. This feature may be absent from COADS-based surface heat flux climatologies because of the strong spatial averaging required in low data regions. In the Atlantic heat flux remains directed downward into the equatorial ocean in spring and fall and directed upward only in winter, reflecting the cooler SSTs of this ocean.

In midlatitudes in both basins net surface heat flux is balanced by local storage. In the North Pacific this balance is nearly perfect, while in the Atlantic convergence of heat transport contributes to 10% to the total heat flux in summertime. Closer to the equator large transport divergences develop in both basins, even as the seasonal cycle of net surface heat flux weakens (see Fig. 5). Descending from 20°N to 15°N the amplitude of the seasonal meridional transports strengthen (Figs. 7a and 8a).

At the lower latitude during winter heat is stored locally in the form of a deepening thermocline, while six months later the thermocline shoals as the warm equatorial water is transported back southward into the equatorial thermocline. Within 15 degrees of the equator large flows of heat in the Pacific follow the solar cycle. In northern summer heat flows southward as a southward gradient of SST develops, while in northern winter heat begins to flow northward, coinciding with a reversal of the SST gradient. The wintertime flow of heat northward exceeds the summertime flow of heat southward so that on average there is a weak northward heat transport in the tropical North Pacific. South of the equator the direction of meridional heat transport is reversed.

The situation in the Atlantic is different. The maximum heat transport occurs at 25°N in the subtropical gyre and has a weak annual cycle with minimum values in the months from January to June. The seasonal change is approximately 0.2 PW. In contrast, several studies (e.g., Molinari et al. 1990; Hsuing et al. 1989) find minimum transport at 26°–27°N in January–February with a seasonal change of 1 PW. At 24°N the seasonal cycle of Ekman transport and compensating deep-water fluxes is small. Thus, at this latitude meridional transport is the result of a small difference between the large seasonal cycle of surface flux and the large rate of local storage (Fig. 5). The rate of heat storage is still positive at midlatitudes in fall, even though the surface input of heat is small or negative. Thus, northward heat transport at 24°N reaches a maximum during this season. This result differs from direct estimates of Molinari et al. (1990) who found a July maximum and indirect estimates of Hsuing et al. (1989) who found maximum transport in spring.

Farther south in the Atlantic the balance of terms in the heat equation [(1)] changes. Surface heat flux and local storage no longer balance as both local storage and transport divergence increase in size. Between 7°N and 15°N storage is negative from June to September. During these months upwelling associated with the northeast trades is at a maximum due to the northward shift of the ITCZ (see, e.g., Carton and Zhou 1997). In this region surface heat flux is generally positive, although small. Thus the horizontal divergence is large, exceeding 5×10^8 W m^{-1}. At 15°N the season of maximum heat transport is December–February as surface heat flux north of this latitude becomes large and negative. Between 7° and 15°N the negative storage in summer causes heat transport to decrease with decreasing latitude until summertime heat transport is nearly zero at 5°N. Meanwhile, south of 7°N downwelling is at its maximum during summer. The increase in heat storage associated with the deepening near-equatorial thermocline exceeds the fairly strong 2.5×10^8–5×10^8 W m^{-1} surface heat input implying near-equatorial heat divergence during the summer, leading to a convergence of heat transport and increases in heat transport farther south.

The results presented above assume that the seasonal cycle itself is stable over multiple decades. We examine this assumption by comparing heat storage and divergence of heat transport computed over the first and second halves of the

analysis period (Fig. 9). The results remain qualitatively the same. Interestingly, the largest differences occur in the phase of heat storage in the North Atlantic north of 30°N, which appears to occur a month earlier in the second half of the record with somewhat reduced amplitude, and in the equatorial Pacific where the seasonal cycle has increased in amplitude.

As discussed in the introduction, several theories have been proposed to explain the presence of strong seasonal variations in heat transport. We begin to address these different mechanisms by considering the deviations of the seasonal heat budget from zonal average:

$$\frac{\partial\{\theta\}}{\partial t} + \frac{\partial\{\mathbf{V}\}\{\theta\}}{\partial y} + \frac{\partial\{\mathbf{V}^*\theta^*\}}{\partial y} = \frac{\{Q\}}{\rho_o C_p} + K_h\{\nabla_h^2\theta\} + \left\{A_v\frac{\partial^2\theta}{\partial z^2}\right\}. \qquad (2)$$

Here, braces indicate zonal averaging and asterisks indicate deviation from zonal average. Following Böning and Hermann (1994) and others we interpret the second and third terms on the left-hand side as divergences of the meridional overturning transport and the horizontal gyre transport. The diffusive term is neglected in our analysis as it only accounts for 1%–2% of the total heat transport.

The results in Figs. 7c,d and Figs. 8c,d show that, annually averaged, the largest term in both oceans is meridional overturning transport except in the subtropical Pacific (20°–35°N). In this range of latitudes gyre transport is similar to the Bryden et al. (1991) estimate at 24°N of 0.38 PW, but the overturning transport is negligible except in January. In the Atlantic gyre transport is significant only between 20° and 30°N where it contributes 30% of the annual northward heat transport. Although our results in the Atlantic seem consistent with the model simulations of Böning and Hermann (1994), and Kobayashi and Imasato (1998), the results of Kamenkovich et al. (2000) do suggest that increasing horizontal resolution will accelerate the horizontal gyre and thus increase heat transport associated with gyre circulation.

Recent direct estimates of heat transport are available along two latitude bands in the Atlantic, 24°–26°N (Baringer and Molinari 1999) and 36°N (Sato and Rossby 2000). Baringer and Molinari find an average southward baroclinic transport based on four transects distributed over four decades of 0.9 ± 0.3 PW. However their estimate does not include transport through the Straits of Florida, and thus is difficult to compare to our estimates. Sato and Rossby were able to estimate the annual cycle of heat transport along 36°N based on 10 transects and found an annual range of 0.6 ± 0.1 PW with much of the uncertainty due to eddy variability, somewhat in excess of the 0.4 PW range we find at this latitude, although within error bars.

In the tropical–subtropical North Pacific recent estimates are also available from 28 transpacific XBT/XCTD transects combined with Ekman transports estimated from European Centre for Medium-Range Weather Forecasts analyses (Roemmich et al. 2001). There the authors conclude that the annual cycle of heat transport is primarily associated with annual changes in Ekman transport, which leads them to an annual range in meridional transport of 1.4 PW with a maximum value in November–December and a minimum value in September. The importance of Ekman transport and thus the September minimum in heat transport is evident in our analysis as well (Fig. 7). However, a direct comparison of the seasonal cycle of heat transport in Fig. 7 is difficult because of the irregular path of the transects.

An alternative way of decomposing the heat budget is to consider deviations from a vertical average. In that case our heat equation becomes

$$\frac{\partial\langle\theta\rangle}{\partial t} + \nabla_h\cdot(\langle\mathbf{V}'\theta'\rangle) + \nabla_h\cdot(\langle\mathbf{V}\rangle\langle\theta\rangle) = \frac{Q}{(\rho_o C_p D)} + K_h\nabla_h^2\langle\theta\rangle, \qquad (3)$$

where angle brackets now indicate averaging over the full depth $D(x, y)$ of the ocean and terms marked with a prime are anomalies from this vertical average. Following Hall and Bryden (1982) we interpret the second and third terms on the left-hand side of (3) as the divergence of baroclinic and barotropic transport (our definition differs from theirs in that they exclude Ekman layer transport). The separate terms are presented in Figs. 7e,f for the Pacific and Figs. 8e,f for the Atlantic. Additional panels (Figs. 7g and 8g) present baroclinic transport in which Ekman layer transport has been removed. It is evident that in the Pacific virtually all of the heat transport is carried out through baroclinic motion. In the

Atlantic the bulk of the transport is baroclinic, but the barotropic transport still accounts for 10% of the total transport.

We next consider the nature of this baroclinic seasonal transport. As indicated in the introduction, Kraus and Levitus (1986) proposed that much of the warm component of this transport occurs in the near-surface layer with compensating cold transport at lower levels. The results based on this approximation, shown in Figs. 7b and 8b are quite comparable to the results presented by Kraus and Levitus and indeed, they do seem to explain much of the seasonal variability of the heat transport (shown in Figs. 7a and 8a). This transport mechanism, which we refer to as Ekman-related transport, is a larger contributor to the total in the North Pacific than it is in the North Atlantic because of the relatively larger importance of the themohaline circulation in the Atlantic. Interestingly the results differ significantly from the simulation-based results of Böning and Herrmann (1994) and Jayne and Marotzke (2000).

In order to determine the range of depths important in determining baroclinic heat transport (Figs. 7 and 8), we introduce the terms accumulated mass and heat transport estimates (Figs. 2 and 3, solid curves). Accumulated mass and heat transport are defined as $\int_z^0 (\int_{\text{west}}^{\text{east}} \rho v \, dx) \, dz$, and $C_p \int_z^0 (\int_{\text{west}}^{\text{east}} \rho v \theta \, dx) \, dz$. When integrated over the full water column the accumulated mass transport is required to be zero by the high latitude boundary conditions of the analysis, and thus the accumulated heat transport becomes the net meridional heat transport discussed earlier. If instead we had allowed a reasonable 0.6 Sv seasonal cycle of upper water transport into the Arctic (Coachman and Aagaard 1988) balanced by deep- and bottom-water transports, this would have introduced a modest increase in meridional heat transport of order 3×10^{13} W m^{-1}.

The results make clear the striking differences in the character of heat transport in the Tropics and midlatitude and between the Pacific and Atlantic. The seasonal distribution of transport in temperature bins clearly determines the seasonal cycle of heat transport in the Tropics (Figs. 2 and 3, middle panels). A dominant part of the seasonal variation in mass transport is associated with wind-driven transport in the mixed layer, as has also been pointed out by Jayne and Marotzke (2001). But it is also clear that the Kraus and Levitus (1986) assumption of uniform flow at depth is too simplistic. In the Pacific at 5°N meridional transports are four to five times stronger in winter than in summer, and they extend much deeper into the water column. This difference in transport explains why the seasonal change of heat transport in the tropical Pacific is so large, ranging from 2 to 6 PW. In the tropical Atlantic similar seasonal changes occur, although their range is more limited.

The contrast between the Tropics and midlatitude is apparent by comparing the results at 5°N with those at 25°N (Figs. 2 and 3, right-hand panels). In the Pacific accumulated heat transport reflects the weak meridional overturning circulation, with northward transport near-surface and at depth and southward transport within the thermocline. Seasonal changes in northward heat transport result from the strengthening in summer of the northward, warm, near-surface flow. In the Atlantic, in contrast, much of the northward transport occurs at depths between 400 and 2000 m and changes little throughout the year with compensating southward transport at depth associated with the southward moving of North Atlantic Deep Water. Thus, we find that the accumulated heat transport contribution from this southward NADW flow is about 0.6 PW, close to the estimate of 0.7 PW of Böning et al. (1996).

4. Conclusions

In this study we compare the heat budgets of the North Atlantic and Pacific Oceans using new results from a reanalysis of ocean circulation for the period 1950–98. Both oceans are forced by westerlies in midlatitude and easterlies in the Tropics. Both have anticyclonic gyre circulations spanning the subtropics and midlatitudes with intense western boundary currents and a set of strong zonal currents in the Tropics. However, the basins differ not only in zonal scale, but also in the presence of deep convection in the North Atlantic.

We find a number of features of the seasonal heat budget in common between the two basins:

- In both basins the local heat storage and heat transport divergence have strong seasonal variations and tend to cancel each other in the Tropics. The transition to a different balance occurs at 15°N. Farther poleward heat transport divergence becomes small and local storage balances surface flux.

- In both basins meridional overturning (which can also be expressed as baroclinic transport, including wind-driven temperature transport) is responsible for most of the mean meridional heat transport. The seasonal variation of heat transport also results mainly from the seasonal variation of meridional overturning (although at different depths in different basins). This result is consistent with some previous studies (Böning and Hermann 1994; Jayne and Marotzke 2001).

We also find a number of differences between the two basins:

- The phase and amplitude of the seasonal cycles are different. Heat transport in the tropical Pacific follows the annual cycle of insolation and as well as the cycle of meridional wind-driven transport so that transport is always directed toward the cooler hemisphere. In the Pacific strong seasonal variations in heat transport divergence occur along the thermal equator (5°N).

  The Atlantic in contrast, has a weaker annual cycle in the deep Tropics reflecting a reduced meridional transport that is semiannual at 15°N. Close to the equator the phase of the seasonal cycle becomes more consistent with the hemispheric shift of solar radiation, but offset so that heat is always transport northward. North of 20°N local storage and surface flux nearly balance (making indirect estimation of seasonal heat transport, which requires differencing these terms, problematic at best).

- The meridional overturning cells that control the seasonal variation of heat transport are different. In the Pacific the vigorous shallow tropical cell has strong seasonal variations, which result in strong seasonal variations of heat transport (5 PW). Fluctuations in either the temperature or velocity of this shallow cell have been implicated in decadal climate fluctuations in the Pacific (Kleeman et al. 1999) raising the interesting possibility of a link between seasonal and decadal variability. Additional studies are necessary to address this.

  In the North Atlantic, the shallow tropical cell is weaker, resulting in smaller seasonal variations in northward heat transport. In midlatitudes southward transport of cold deep water balances the northward transport of warm thermocline water (much of this northward transport is occurring in the Gulf Stream).

The applicability of these results to the ocean depends on the accuracy of the reanalysis, an issue mainly addressed elsewhere. Last, although we have focused on seasonal variations in the heat budget, year-to-year variations may be considerable. Determination of these variations and their link to climate is the focus of our ongoing work.

Acknowledgments

We gratefully acknowledge the support of the National Science Foundation (Grants OCE9530220 and OCE9812404) for this work. We would like to thank two anonymous reviewers for their extensive helpful comments. This work forms part of the dissertation research of JW.

REFERENCES

Baringer M. O., and R. Molinari, 1999: Atlantic Ocean baroclinic heat flux at 24° to 26°N. *Geophys. Res. Lett.*, **26**, 353–356. Find this article online

Baringer M. O., and J. C. Larsen, 2001: Sixteen years of Florida Current transport at 27N. *Geophys. Res. Lett.*, **28**, 3173–3182. Find this article online

Blanc T. V., 1985: Variation of bulk-derived surface flux, stability, and roughness results due to the use of different transfer coefficient schemes. *J. Phys. Oceanogr.*, **15**, 650–669. Find this article online

Böning C. W., and P. Herrmann, 1994: Annual cycle of poleward heat transport in the ocean: Results from high resolution modeling of the North and equatorial Atlantic. *J. Phys. Oceanogr.*, **24**, 91–107. Find this article online

Böning C. W., W. R. Holland, F. O. Bryan, G. Danabasoglu, and J. C. McWilliams, 1995: An overlooked problem in model simulations of the thermocline circulation and heat transport in the Atlantic Ocean. *J. Climate*, **8**, 515–523. Find this article online

Böning C. W., F. O. Bryan, and W. R. Holland, 1996: Deep-water formation and meridional overturning in a high-resolution model of the North Atlantic. *J. Phys. Oceanogr.*, **26**, 1142–1164. Find this article online

Bryan K., 1962: Measurements of meridional heat transport by ocean currents. *J. Mar. Res.*, **67**, 3403–3413. Find this article online

Bryden H. L., and M. M. Hall, 1980: Heat transport by currents across 25°N latitude in the Atlantic Ocean. *Science*, **207**, 884–886. Find this article online

Bryden H. L., D. H. Roemmich, and J. A. Church, 1991: Ocean heat transport across 24°N in the Pacific. *Deep-Sea Res.*, **38**, 297–324. Find this article online

Bunker A. F., 1976: A computation of surface energy flux and annual cycle of the North Atlantic Ocean. *Mon. Wea. Rev.*, **104**, 1122–1140. Find this article online

Carton J. A., and Z. Zhou, 1997: Annual cycle of sea surface temperature in the tropical Atlantic Ocean. *J. Geophys. Res.*, **102**, 27813–27824. Find this article online

Carton J. A., G. Chepurin, X. Cao, and B. S. Giese, 2000a: A simple ocean data assimilation analysis of the global upper ocean 1950–1995. Part I: Methodology. *J. Phys. Oceanogr.*, **30**, 294–309. Find this article online

Carton J. A., G. Chepurin, and X. Cao, 2000b: A simple ocean data assimilation analysis of the global upper ocean 1950–1995. Part II: Results. *J. Phys. Oceanogr.*, **30**, 311–326. Find this article online

Chepurin G., and J. A. Carton, 1999: Comparison of retrospective analyses of the global ocean heat content. *Dyn. Atmos. Oceans*, **29**, 119–145. Find this article online

Coachman L. K., and K. Aagaard, 1988: Transports through Bering Strait: Annual and interannual variability. *J. Geophys. Res.*, **93**, 15535–15539. Find this article online

da Silva A. M., and S. Levitus, 1994: *Algorithms and Procedures*. Vol. 1, *Atlas of Surface Marine Data*, NOAA Atlas NESDIS 1, 83 pp.

da Silva A. M., C. C. Young, and S. Levitus, 1994: *Algorithms and Procedures*. Vol. 2, *Atlas of Surface Marine Data*, NOAA Atlas NESDIS 2, 83 pp.

Esbensen S. K., and V. Kushnir, 1981: The heat budget of the global ocean: An atlas based on estimates from surface marine observations. Climate Research Institute Rep. No. 29, Oregon State University, 27 pp. [Available from College of Oceanic and Atmospheric Sciences, Oregon State University, Corvallis, OR 97331.].

Fillenbaum E. R., and T. N. Lee, 1997: Meridional heat transport variability at 26.5°N in the Atlantic. *J. Phys. Oceanogr.*, **27**, 153–174. Find this article online

Gleckler P. J., and B. Weare, 1997: Uncertainties in global ocean surface heat flux climatologies derived from ship observations. *J. Climate*, **10**, 2763–2781. Find this article online

Hall M. M., and H. L. Bryden, 1982: Direct estimates and mechanisms of ocean heat transport. *Deep-Sea Res.*, **29**, 339–359. Find this article online

Hastenrath S., 1982: On meridional heat transport in the world ocean. *J. Phys. Oceanogr.*, **12**, 922–927. Find this article online

Holland W. R., and F. O. Bryan, 1994: Sensitivity studies on the role of the ocean in climate change. *Ocean Processes in Climate Dynamics: Global and Mediterranean Example*, P. Malanotte-Rizzoli and A. R. Robinson, Eds., Kluwer Academic, 111–134.

Hsiung J., 1985: Estimate of global oceanic meridional heat transport. *J. Phys. Oceanogr.*, **15**, 1405–1413. Find this article online

Hsiung J., R. E. Newell, and T. Houghtby, 1989: The annual cycle of heat storage and ocean meridional heat transport. *Quart. J. Roy. Meteor. Soc.*, **115**, 1–28. Find this article online

Jayne S. R., and J. Marotzke, 2000: The dynamics of ocean heat transport variability. *Int. WOCE Newslett.*, No. 38, WOCE International Project Office, Southampton, United Kingdom, 7–9.

Jayne S. R., and J. Marotzke, 2001: The dynamics of ocean heat transport. *Rev. Geophys.*, **39**, 385–411. Find this article online

Johnson G. C., 2001: The Pacific Ocean subtropical cell surface limb. *Geophys. Res. Lett.*, **28**, 1771–1774. Find this article online

Johnson G. C., and M. J. McPhaden, 1999: Interior pycnocline flow from the subtropical to the equatorial Pacific Ocean. *J. Phys. Oceanogr.*, **29**, 3073–3089. Find this article online

Jung G. H., 1952: Note on the meridional transport of energy by the ocean. *J. Mar. Res.*, **11**, 139–146. Find this article online

Kamenkovich I., J. Marotzke, and P. H. Stone, 2000: Factors affecting heat transport in an ocean general circulation model. *J. Phys. Oceanogr.*, **30**, 175–194. Find this article online

Kleeman R., J. P. McCreary, and B. A. Klinger, 1999: A mechanism for generating ENSO decadal variability. *Geophys. Res. Lett.*, **26**, 1743–1746. Find this article online

Kobayashi T., and N. Imasato, 1998: Seasonal variability of heat transport derived from hydrographic and wind stress data. *J. Geophys. Res.*, **103**, 24663–24674. Find this article online

Kraus E. B., and S. Levitus, 1986: Annual heat flux variations across the tropic circles. *J. Phys. Oceanogr.*, **16**, 1479–1486. Find this article online

Lamb P., and A. F. Bunker, 1982: The annual march of the heat budget of the North and tropical Atlantic Ocean. *J. Phys. Oceanogr.*, **12**, 1388–1410. Find this article online

Levitus S., and J. Antonov, 1997: *Climatological and Interannual Variability of Temperature, Heat Storage, and Rate of Heat Storage in the Upper Ocean*. NOAA Atlas NESDIS 16, 6 pp.

MacDonald A. M., and C. Wunsch, 1996: An estimate of global ocean circulation and heat fluxes. *Nature*, **382**, 436–439. Find this article online

Moisan J. R., and P. P. Niiler, 1998: The seasonal heat budget in the North Pacific, net heat flux and heat storage rates (1950–1990). *J. Phys. Oceanogr.*, **28**, 401–420. Find this article online

Molinari R. L., E. Johns, and J. F. Festa, 1990: The annual cycle of meridional heat flux in the Atlantic Ocean at 26.5°N. *J. Phys. Oceanogr.*, **20**, 476–482. Find this article online

Oberhuber J. M., 1988: An atlas based on the 'COADS' data set: The budget of heat, buoyancy and turbulent kinetic energy at the surface of the global ocean. Rep. 15, Max Planck Institute for Meteorology, 20 pp.

Oort A. H., and T. Vonder Haar, 1976: On the observed annual cycle in the ocean–atmosphere heat balance over the Northern Hemisphere. *J. Phys. Oceanogr.*, **6**, 781–800. Find this article online

Philander S. G. H., and R. C. Pacanowski, 1986: The mass and heat budget in a model of the tropical Atlantic Ocean. *J. Geophys. Res.*, **91**, 3293–3303. Find this article online

Reynolds R. W., and T. M. Smith, 1994: Improved global sea surface temperature analysis using optimum interpolation. *J. Climate*, **7**, 929–948. Find this article online

Roemmich D., J. Gilson, and B. Cornuelle, 2001: Mean and time-varying meridional transport of heat at the tropical–subtropical boundary in the North Pacific Ocean. *J. Geophys. Res.*, **106**, 8957–8970. Find this article online

Sato O. T., and T. Rossby, 2000: Seasonal and low-frequency variability of meridional heat flux at 36°N in the North Atlantic. *J. Phys. Oceanogr.*, **30**, 606–620. Find this article online

Schmitz W. J. Jr.,, and P. L. Richardson, 1991: On the North Atlantic circulation. *Rev. Geophys.*, **31**, 29–49. Find this article online

Talley L. D., 1984: Meridional heat transport in the Pacific Ocean. *J. Phys. Oceanogr.*, **14**, 231–241. Find this article online

Trenberth K. E., and J. M. Caron, 2001: Estimates of meridional atmosphere and ocean heat transport. *J. Climate*, **14**, 3433–3443. Find this article online

Wang W., and M. J. McPhaden, 2000: The surface-layer heat balance in the equatorial Pacific Ocean. *J. Phys. Oceanogr.*, **30**, 2989–3008. Find this article online

Wijffels S. E., J. M. Toole, H. L. Bryden, R. A. Fine, W. J. Jenkins, and J. L. Bullister, 1996: The water masses and circulation at 10N in the Pacific. *Deep-Sea Res.*, **43**, 501–544. Find this article online

Wilkin J. L., J. V. Mansbridge, and J. S. Godfrey, 1995: Pacific Ocean heat transport at 24°N in a high-resolution global model. *J. Phys. Oceanogr.*, **25**, 2204–2214. Find this article online

Yu L., and P. Malanotte-Rizzoli, 1998: Inverse modeling of seasonal variations in the North Atlantic Ocean. *J. Phys. Oceanogr.*, **28**, 902–922. Find this article online

---

Figures

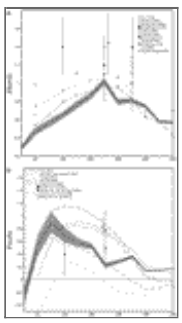

Click on thumbnail for full-sized image.

FIG. 1. Zonally and vertically integrated time mean northward heat transport for the North Pacific and Atlantic Oceans. Shading indicates the standard errors associated with the limited 49-yr sampling record. The large, unknown error, due to bias is not included in this estimate (unit is PW)

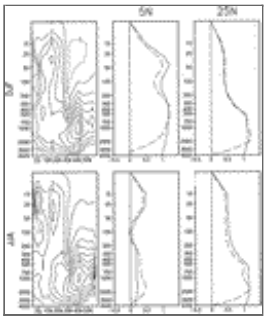

Click on thumbnail for full-sized image.

FIG. 2. Seasonal mean meridional overturning streamfunction (left panels, contour interval is 3 Sv) and accumulated mass and heat transport (middle and right panels; solid line, accumulated heat transport in PW, dash line, accumulated mass transport in units of 10 Sv) at 5°N and 25°N in Atlantic. Accumulated mass and heat transports are defined as $\int_z^0 (\int_{\text{west}}^{\text{east}} \rho v \, dx) \, dz$, and $C_p \int_z^0 (\int_{\text{west}}^{\text{east}} \rho v T \, dx) \, dz$

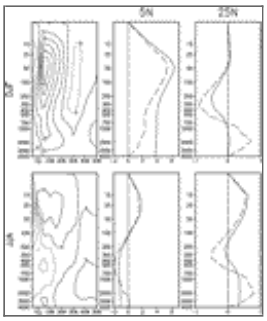

Click on thumbnail for full-sized image.

FIG. 3. As in Fig. 2 except for the Pacific. Contour interval is 9 Sv

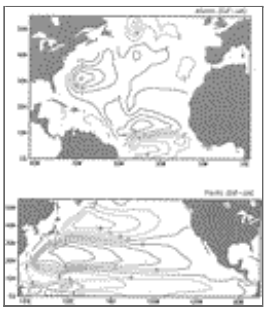

Click on thumbnail for full-sized image.

FIG. 4. Seasonal variation in barotropic volume transport for the Pacific and Atlantic. Contour intervals are 2 and 6 Sv for Atlantic and Pacific, respectively

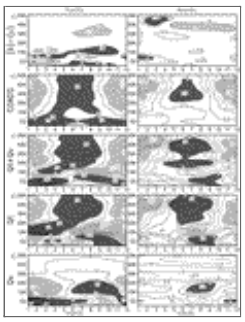

Click on thumbnail for full-sized image.

FIG. 5. Zonally and vertically integrated monthly heat budget for the (left) Pacific and (right) Atlantic. (a) Difference between (b)

and (c). (b) Observed surface heat flux (da Silva and Levitus 1994). The uncertainty in these estimates is approximately 5×10^8 W m^{-1} in the tropical Pacific and one-third of that in the tropical Atlantic (see text for discussion). (c) Sum of heat storage and horizontal divergence of heat flux. (d) Heat storage. (e) Horizontal divergence of heat flux. Contour intervals are 5×10^8 W m^{-1} (Pacific) and 2.5×10^8 W m^{-1} (Atlantic). Zero contours are not drawn in (a)

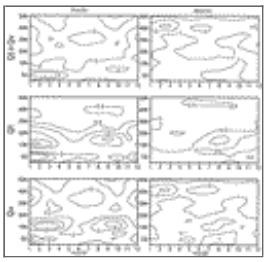

Click on thumbnail for full-sized image.

FIG. 6. Standard error of monthly heat budget for Pacific and Atlantic corresponding to Fig. 5. Standard error is computed from the standard deviation of monthly estimates from their climatological monthly cycle assuming that each year represents an independent estimate. Units are 10^8 W m^{-1}

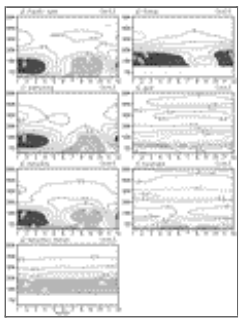

Click on thumbnail for full-sized image.

FIG. 7. Seasonal cycle of heat transport in Pacific: (a) total heat transport, (b) Ekman transport, (c) meridional overturning transport, (d) horizontal gyre transport, (e) baroclinic transport, (f) barotropic transport, and (g) baroclinic − Ekman transport. Contour intervals are labeled at upper-right corners of each panel. Values less than −1 or greater than 2 PW are shaded

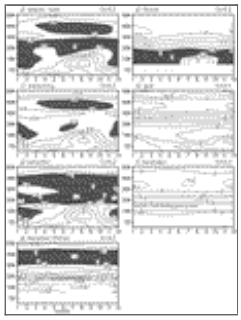

Click on thumbnail for full-sized image.

FIG. 8. As in Fig. 7 except for the Atlantic. Values exceeding ±0.8 PW are shaded

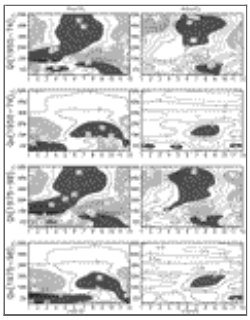

Click on thumbnail for full-sized image.

FIG. 9. Zonally and vertically integrated monthly (a), (c) heat storage and (b), (d) divergence of heat transport for the (left) Pacific and (right) Atlantic over the first half (1950–74, upper two panels) and second half (1975–98, lower two panels) of the analysis period. Contour intervals are 5×10^8 W m^{-1} (Pacific) and 2.5×10^8 W m^{-1} (Atlantic)

* Current affiliation: Center for Ocean–Land–Atmosphere Studies, Calverton, Maryland

Corresponding author address: James A. Carton, Department of Meteorology, University of Maryland at College Park, 3433 Computer and Space Science Building, College Park, MD 20742. E-mail: carton@atmos.umd.edu

[1] The uncertainties in estimates of surface heat flux derived from bulk formulas are discussed in many recent papers including da Silva et al. (1994) who identify an average 30 W m^{-2} heat flux imbalance. Gleckler and Weare (1997) find uncertainties in the zonal mean latent heat flux to range from 10–20 W m^{-2} in the Tropics to 30 W m^{-2} in midlatitudes. Uncertainties in solar flux alone exceed 25 W m^{-2} throughout the Tropics. Wang and McPhaden (2000) present direct comparisons of the flux seasonal cycle with estimates from the TOGA/TAO buoys in the tropical Pacific and find differences that can reach 50 W m^{-2}. Thus the uncertainties in estimates of surface heat flux based on bulk formulas are considerable.

top